NASA CONTRACTOR REPORT

NASA CR-155

NASA CR-155

SPACECRAFT TEMPERATURE CONTROL BY THERMOSTATIC FINS-ANALYSIS

PART II

by J. A. Wiebelt, J. F. Parmer, and G. J. Kneissl

Prepared under Grant No. NsG-454 *by*
OKLAHOMA STATE UNIVERSITY
Stillwater, Okla.
for

NATIONAL AERONAUTICS AND SPACE ADMINISTRATION • WASHINGTON, D. C. • JANUARY 1965

SPACECRAFT TEMPERATURE CONTROL BY THERMOSTATIC FINS-ANALYSIS

Part II

By J. A. Wiebelt, J. F. Parmer, and G. J. Kneissl

Prepared under Grant No. NsG-454 by
OKLAHOMA STATE UNIVERSITY
Stillwater, Oklahoma

for

NATIONAL AERONAUTICS AND SPACE ADMINISTRATION

For sale by the Office of Technical Services, Department of Commerce,
Washington, D.C. 20230 -- Price $2.00

INTRODUCTION

Review

In the December, 1963 Interim Report,[1]* the basic analysis and design configuration for a new method of spacecraft temperature control was presented. The basic configuration described is shown in Fig. 1. The fins are bimetallic strips which change their radius of curvature as a function of spacecraft skin temperature, which is a function of solar azimuth and zenith angles. This change in curvature effectively regulates the average α_s/e_t ratio of the surface which is sufficient to provide active control of the spacecraft temperature [1]. The descriptive parameter which is used to determine the thermostatic surfaces effectiveness is e'_r, where

$$e'_r = q''/\sigma T_s^4 = e_t - \alpha_s \frac{G_s}{\sigma T_s^4} \qquad (1)$$

in which

- q'' is the net radiation heat flux for the surface Btu/hr-ft^2
- σ is the Stefan-Boltzman constant $.1714 \times 10^{-8}$ Btu/hr-ft^2-$^\circ$R^4
- T_s is the temperature of the surface ($^\circ$R)
- e_t is the average terrestial emittance of the surface
- α_s is the average solar absorptance of the surface
- G_s is the solar irradiation

This parameter e'_r was evaluated for fin height to spacing distance ratios of .667, 1, and 2 inches/inch assuming that the fin lengths were infinite in extent, and nonemitting. Monochromatic analysis, on the spectral properties of the fin and spacecraft skin materials, was used to determine e_t and α_s. [1]

---

*Numbers in brackets refer to the bibliography listed at the end of this report.

NASA SPACECRAFT THERMOSTAT SURFACE

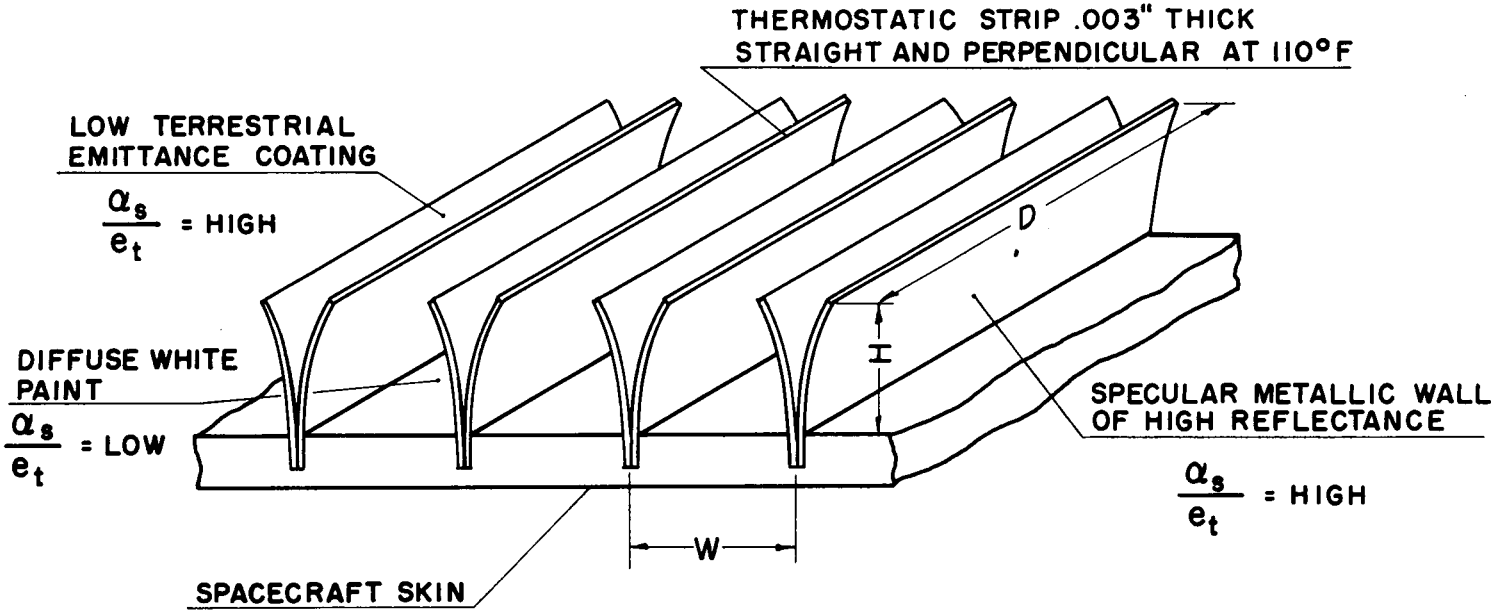

Figure (1)

For this report, the analytical work was extended to include the case of finite length surfaces with either emitting or nonemitting fins. In addition to the basic analytical work, an integrating sphere reflectometer was constructed so that the reflective properties of the thermostatic fins could be measured. Also, a full size model of the spacecraft surface system was designed and is presently under construction. This model was designed for testing in a space simulator at Goddard Laboratory. A test model of the surface is shown in Fig. 2.

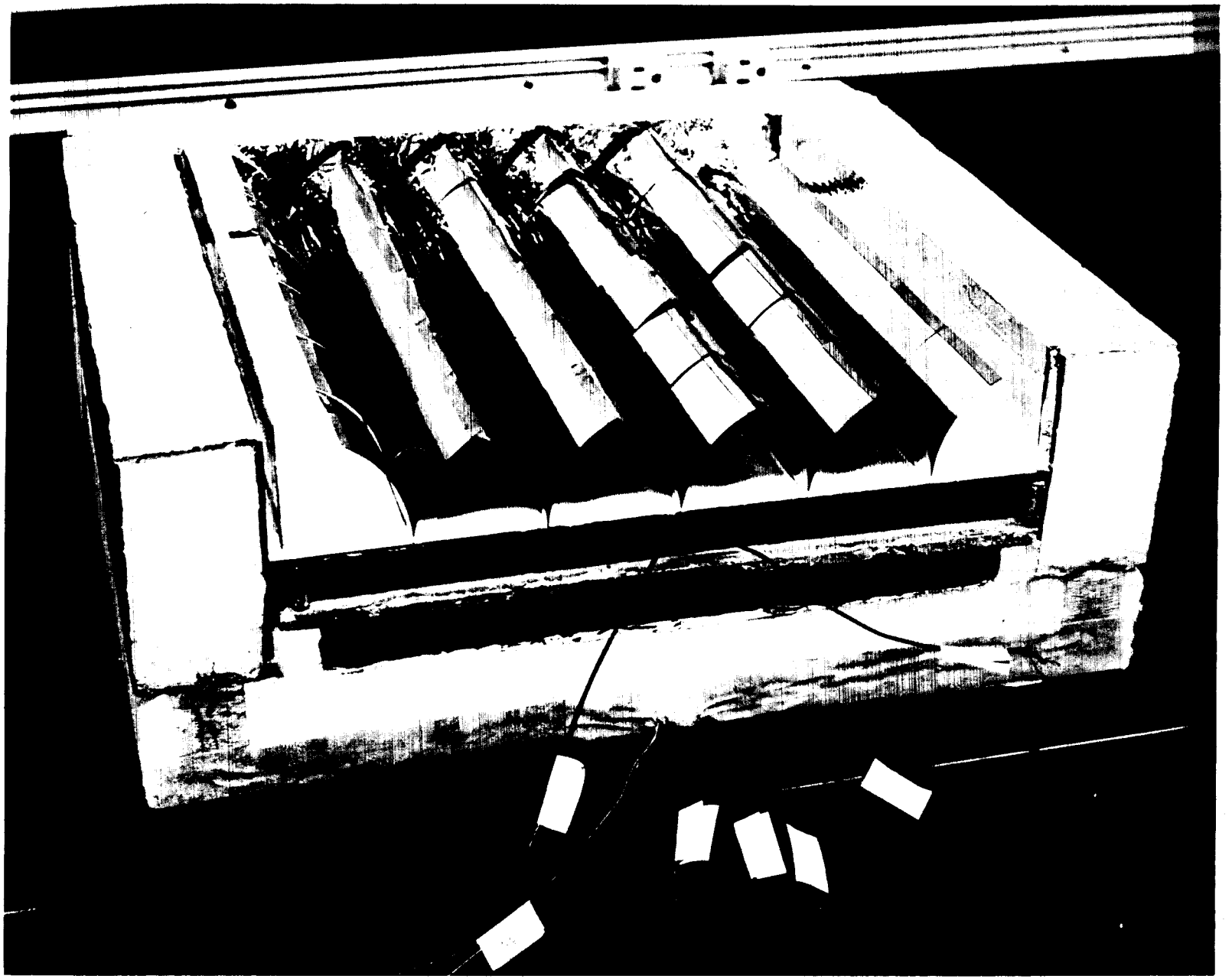

Figure (2) Demonstration surface--closed position

ANALYSIS

Calculation of Effective Reflectance of a Finite Length Groove with Specular Sides and a Diffuse Bottom

Assumptions
1) Specular Vertical Walls
2) Diffuse Horizontal Base
3) Finite Length Grooves with Open Ends
4) Azimuth Angle of Irradiation Perpendicular to the Walls.
5) Solar Irradiation, i.e., parallel rays incoming from the sun

Since the surface is assumed to be irradiated by parallel rays from the sun, such that the azimuthal angle with respect to the wall is zero, a certain fraction of the incoming energy will be absorbed by interreflections between the specular walls, the number of reflections being a function of the solar polar angle φ and the height to width ratio H/W.

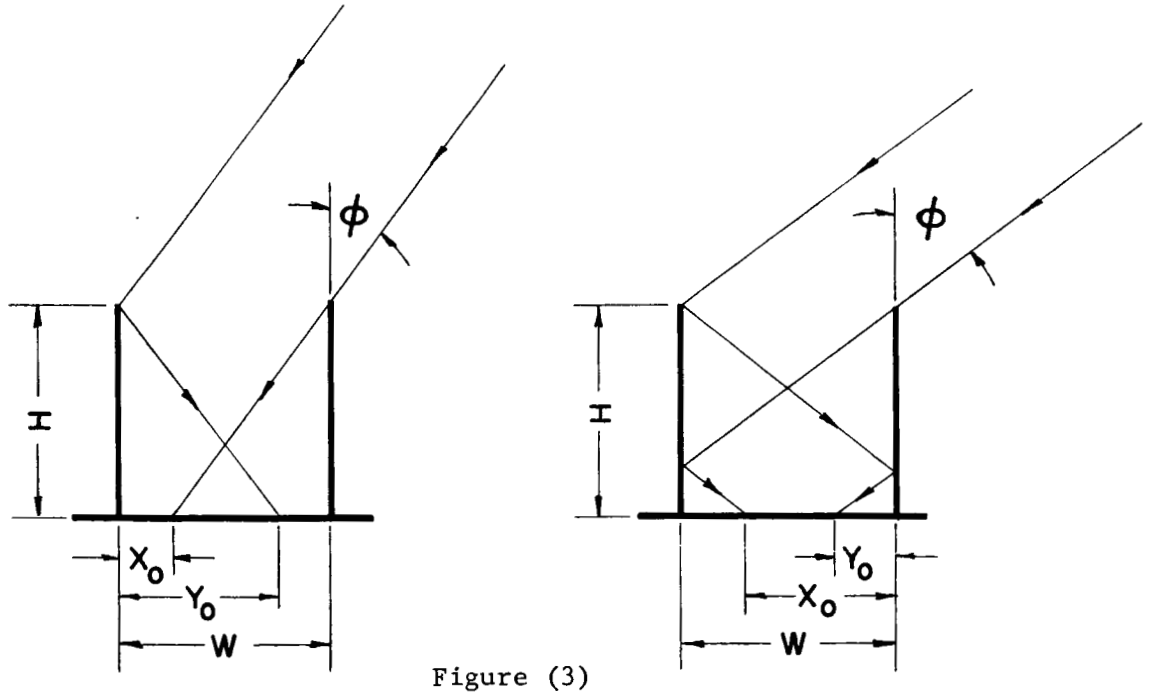

Figure (3)

Due to multiple reflections from the specular walls, the base is irradiated in two discrete sections. This is illustrated in Fig. 3. Since the total energy leaving the system is the quantity required in the calculation, the energy leaving due to each of the two discrete areas, A_{o-x_o} and A_{o-y_o}, can be calculated separately and then summed. Since the areas are geometrically similar, the irradiation of the areas can be expressed mathematically.

When placed in a solar environment with solar polar angle φ between arctan (mW/H) and arctan (nW/H), where (m,n) = (0,1),(1,2) . . . (m,m+1), . . the irradiation of areas $A_{o-x_o} = x_o D$ and $A_{o-y_o} = y_o D$ are respectively:

$$I_{x_o} = S \cos\varphi \, (\rho_w)^m \text{ Btu/hr-ft}^2 \tag{2}$$

$$I_{y_o} = S \cos\varphi \, (\rho_w)^n \text{ Btu/hr-ft}^2 \tag{3}$$

where S = the solar constant 442 Btu/hr-ft^2,
$\cos\varphi$ accounts for the reduction in projected area which receives the sun's energy and $(\rho_w)^m$ accounts for the energy absorbed in the successive reflections.

The radiosities of A_{o-x_o} and A_{o-y_o} are:

$$J_{x_o} = \rho_b I_{x_o} \tag{4}$$

$$J_{y_o} = \rho_b I_{y_o} \tag{5}$$

ρ_w = the reflectance of the wall material

ρ_b = the reflectance of the base material.

Effective Reflectance

The effective reflectance of the spacecraft surface is defined as the ratio of the energy which finally escapes from the surface to the energy which originally struck the surface. The energy which escapes is equal to the sum of the radiosities of the two sections, A_{o-x_o} and A_{o-y_o} minus the fraction of this energy which is absorbed by the wall material. This is because the base does not see itself or any of its images in the vertical walls of the groove. With this assumption,

$$\rho_e = \frac{A_{x_o} J_{x_o} (1 - \alpha_w F_{x_o -w}) + A_{y_o} J_{y_o} (1 - \alpha_w F_{y_o -w})}{WDS \cos\varphi} \quad (6)$$

or in terms of the irradiation

$$\rho_e/\rho_b = \frac{A_{x_o} I_{x_o} (1 - \alpha_w F_{x_o -w}) + A_{y_o} I_{y_o} (1 - \alpha_w F_{y_o -w})}{WDS \cos\varphi} \quad (7)$$

where $F_{x_o -w}$ = the fraction of the energy leaving A_{x_o} which is incident upon the walls of the groove including energy which has undergone multiple reflections between the walls.

W = the distance between fins

D = the length of the groove.

Fig. 4 illustrates how the multiple reflection by the specular walls cause the incident energy on the walls to appear to come from an infinite series of virtual images of the base in the walls.

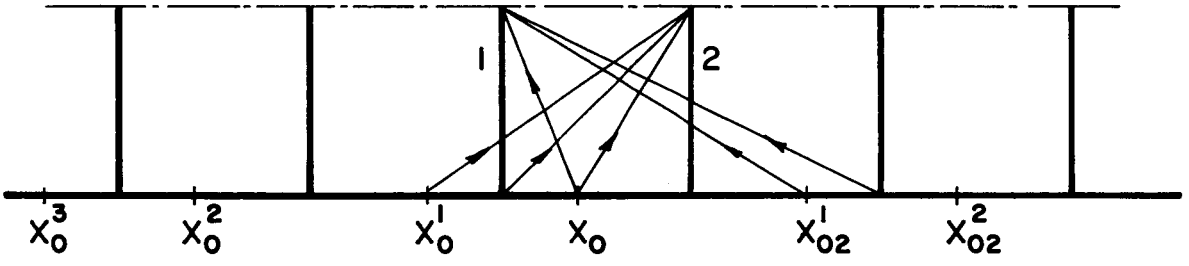

Figure (4)

$F_{x_o -w}$ is then composed of both direct radiation and reflected radiation The amount of reflected radiation being dependent not only upon the geometric configuration of the groove but also upon the reflectance of the specular walls.

$F_{x_o -w}$ is given by the formula:

$$F_{x_o -w} = F_{x_o -1} + F_{x_o -2} + \rho_w (F_{x_o' -1} + F_{x_o' -2})$$

$$+ \rho_w^2 (F_{x_o'' -1} + F_{x_o'' -2}) + \ldots\ldots$$

$$= \sum_{n=0}^{\infty} \rho_w^n \left(F_{x_o^n -1} + F_{x_o^n -1} \right) \quad (8)$$

wherein the individual view factors on the right hand side are calculated by means of geometric flux algebra according to the geometry of Fig. 5.

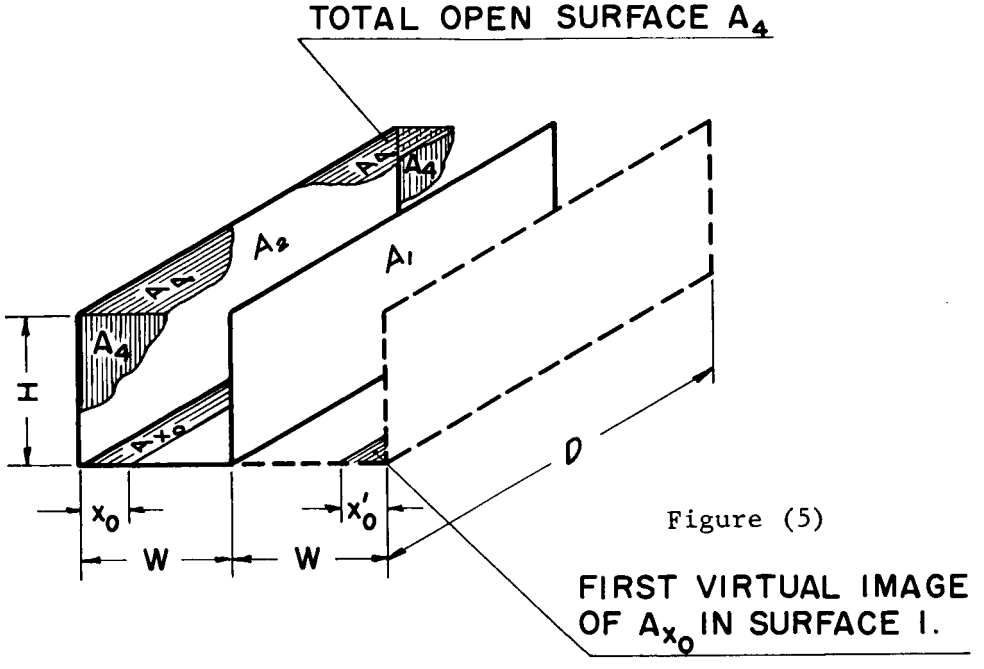

Figure (5)

For example

$$F_{x'_o-2} = \frac{A_{2w}F_{2w-2} - A_{2w-x_o}F_{(2w-x)_o-2}}{A'_{x_o}} \tag{9}$$

where

$$A_{2w} = 2WD$$

$$A_{2w-x_o} = (2W - x_o)D$$

and

$$F_{2w-2} = \frac{1}{\pi L}\left(L \tan^{-1}\left(\frac{1}{L}\right) + N \tan^{-1}\left(\frac{1}{N}\right) - \sqrt{N^2 + L^2}\tan^{-1}\frac{1}{\sqrt{N^2 + L^2}}\right. \tag{10}$$

$$\left. + \frac{1}{4}\log_e\left\{\left[\frac{(1+L^2)(1+N^2)}{1+N^2+L^2}\right]\left[\frac{L^2(1+L^2+N^2)}{(1+L^2)(L^2+N^2)}\right]^{L^2}\left[\frac{N^2(1+L^2+N^2)}{(1+N^2)(L^2+N^2)}\right]^{N^2}\right\}\right)$$

in which $L = \frac{2W}{D}$ and $B = \frac{H}{D}$, see reference [2]. The results of these calculations are shown graphically in Figs. 6 and 7.

Calculation of Effective Emittance Factors

If the fins are assumed to be at 0°R, the effective emittance of the surface is equal to the emittance of the base less that fraction of the energy emitted which is absorbed by the walls. This quantity is given by the reflectance ratio ρ_e/ρ_b evaluated at a solar polar angle of $\varphi = 0$ for any given wall reflectance. This is easily seen from the following manipulation of Eq. (6).

At $\varphi = 0$, $y_o = 0$,

$$\text{and therefore } \rho_e = \frac{WD\, J_{x_o}\, (1 - \alpha_w F_{x_o\text{-}w})}{S(\cos\varphi)\, WD}$$

$$\text{but } J_{x_o} = S\, \rho_b$$

$$\text{thus } \rho_e = \rho_b(1 - \alpha_w F_{x_o\text{-}w}) \tag{11}$$

$$\text{and } \frac{\rho_e}{\rho_b} = 1 - \alpha_w F_{x_o\text{-}w} \text{ at } \varphi = 0 \tag{12}$$

By definition the effective emittance factor of the surface is the energy leaving the surface because of the thermal emission of the surface divided by the black body radiation at the surface temperature.

$$\text{So } e_{ef} = q/E_{bTs}$$

$$\text{where } q = e_{ef}A_b\, \sigma T_b^4 = e_b A_b\, \sigma T_b^4 - e_b A_b\, \sigma T_b^4\, \alpha_w F_{x_o\text{-}w}$$

$$\text{thus } e_{ef} = e_b(1 - \alpha_w F_{x_o\text{-}w}) = e_b \left.\frac{\rho_e}{\rho_b}\right|_{\varphi=0} \tag{13}$$

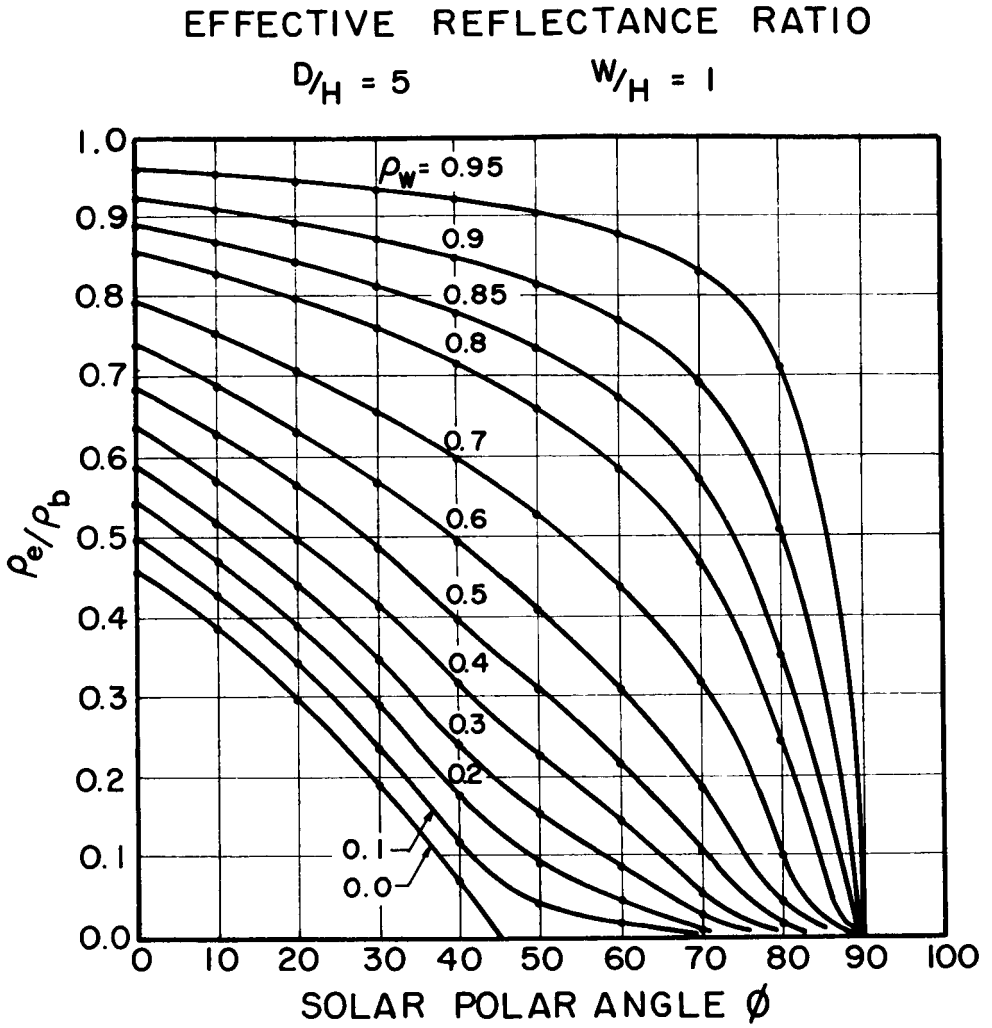
EFFECTIVE REFLECTANCE RATIO
D/H = 5
W/H = 1
ρw = 0.95
0.9
0.85
0.8
0.7
0.6
0.5
0.4
0.3
0.2
0.1
0.0
ρe/ρb
1.0
0.9
0.8
0.7
0.6
0.5
0.4
0.3
0.2
0.1
0.0
0
10
20
30
40
50
60
70
80
90
100
SOLAR POLAR ANGLE Ø

Figure (6)

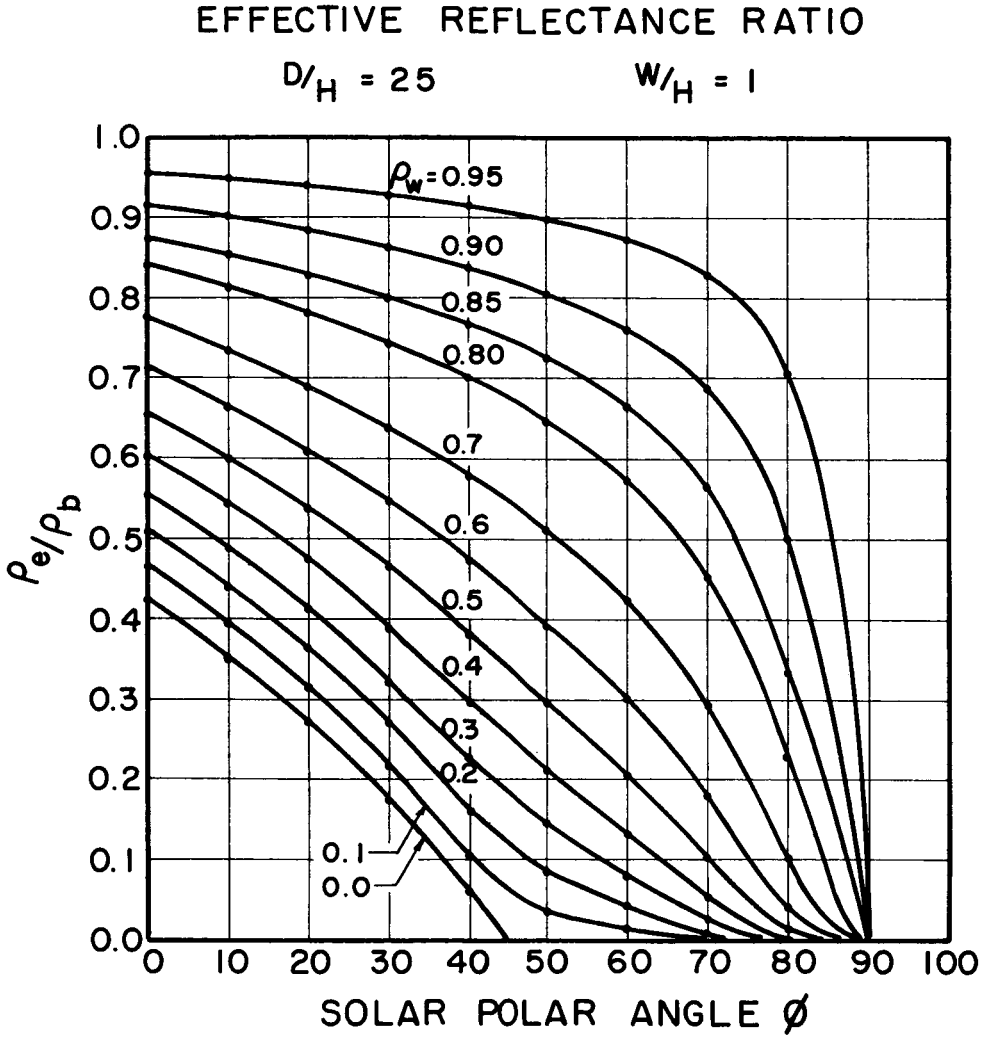
EFFECTIVE REFLECTANCE RATIO
D/H = 25
W/H = 1
ρw=0.95
0.90
0.85
0.80
0.7
0.6
0.5
0.4
0.3
0.2
0.1
0.0
ρe/ρb
1.0
0.9
0.8
0.7
0.6
0.5
0.4
0.3
0.2
0.1
0.0
0 10 20 30 40 50 60 70 80 90 100
SOLAR POLAR ANGLE Ø

Figure (7)

If the fins are at the same temperature as the base then their emission must be taken into consideration also.

The equation for the heat lost from the finite length thermostat surface with fins at the temperature of the base becomes:

$$q_T = 2A_2 e_2 \sigma T^4 F_{(2-4)T} + A_b e_b \sigma T^4 F_{(b-4)T} \tag{14}$$

$$= e_{ef} \sigma T^4 A_b = 2A_2 e_2 \sigma T^4 \left[1 - F_{22}\alpha_2 - F_{23}\alpha_3 - F_{2b}\alpha_b - \rho_b F_{21}(1 - F_{(b-4)T}) \right] + e_1 A_b \sigma T^4 F_{(b-4)T} \tag{15}$$

$$e_{ef} = 2 \frac{A_2}{A_b} e_2 \left[1 - F_{22}\alpha_2 - F_{23}\alpha_3 - F_{2b}\alpha_b - \rho_b F_{21}(1-F_{(b-4)T}) \right] + e_1 F_{(b-4)T} \tag{16}$$

where F_{22} and F_{23} are the fractions of energy from 2 directly incident upon 2 or 3 plus the energy incident due to multiple reflections. The other F factors are similarly defined. This results in $F_{23} = F_{32}$, $F_{22} = F_{33}$, and $F_{2b} = F_{3b}$ by symmetry.

Some of the configuration factors are known from the previous calculations for effective reflectance.

$$F_{(b-4)T} = 1 - 2\alpha F_{(b-2)T} \tag{17}$$

where $F_{(b-2)T}$ is known from Eq. (8) in which $x_o = W$ at $\varphi = 0$. By reciprocity

$$A_b F_{(b-2)T} = A_2 F_{(2-b)T} \tag{18}$$

$$F_{(2-b)T} = \frac{A_b}{A_2} F_{(b-2)T} \tag{19}$$

The view factor $F_{(2-4)T}$ is a little harder to calculate. It involves the calculation of a view factor between specular surfaces. The procedure is as follows:

From the geometry of Fig. 8,

$$1 = F_{(2\text{-}4)T} + F_{(2\text{-}3)T} + F_{(2\text{-}2)T} + F_{(2\text{-}b)T}$$

$F_{(2\text{-}b)T}$ is known from the previous calculation and $F_{(2\text{-}3)T}$ is the sum of the first direct view factor from 2 to 3 plus the sum of the view factors from the virtual images of 2 in 2 to surface 3, each multiplied by $\rho_w^{\,n}$ where n is the number of reflections each virtual image must undergo.

$F_{(2\text{-}2)T}$ is the sum of the view factors from the virtual images of 2 in 3 to surface 2 multiplied by $\rho_w^{\,n}$.

Then $$F_{(2\text{-}3)T} = F_{23} + \rho_w^{\,2} F_{2''\text{-}3} + \rho_w^{\,4} F_{2''''\text{-}3} + \ldots \qquad (20)$$

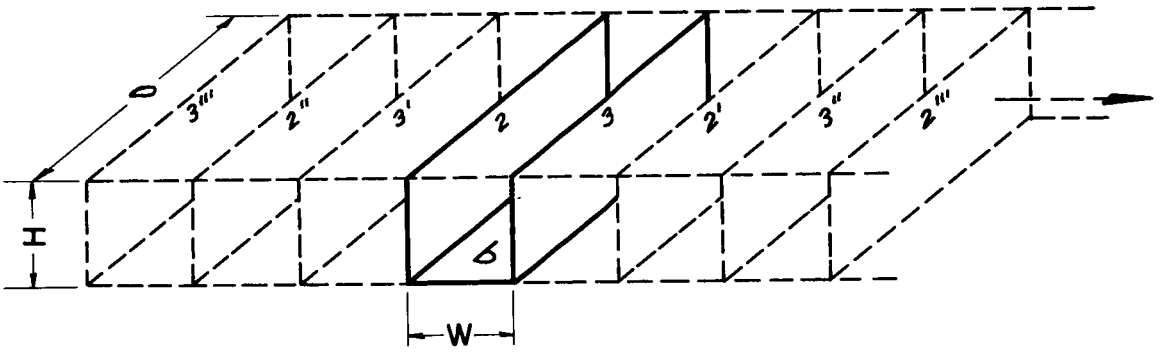

Figure (8)

and $$F_{(2\text{-}2)T} = \rho_w F_{2'\text{-}2} + \rho_w^{\,3} F_{2'''\text{-}2} + \ldots \qquad (21)$$

Where the view factor between any two parallel opposing images has the value

$$F_{2^n\text{-}3} = \frac{2}{\pi xy}\left\{\log_e \frac{(1+x^2)(1+y^2)}{1+x^2+y^2} + y\sqrt{1+x^2}\,\tan^{-1}\frac{y}{\sqrt{1+x^2}} + x\sqrt{1+y^2}\,\tan^{-1}\frac{x}{\sqrt{1+y^2}} - y\tan^{-1}(y) - x\tan^{-1}(x)\right\}\rho_w^{\,n} \qquad (22)$$

in which

$$X = \frac{D}{Wn} \text{ and } Y = \frac{H}{Wn} \quad [2] \qquad (23)$$

The effective emittance factor as calculated from Eq. (16) is shown in Figs. 9 and 10.

Once the effective reflectance ratio and emittance factor for a particular fin configuration is known it is possible to calculate the monochromatic reflection characteristics of the surface as a function of solar polar angle and also calculate the monochromatic emittance factor of the surface. The effective monochromatic reflectance and emittance factor curves are different because the surface is irradiated specularly while it emits diffusely.

The equations for the calculation of reflectance and emittance factor are from the well known relations

$$\rho_e(\varphi) = \frac{\int_0^\infty \rho_\lambda(\varphi) E_{b\lambda} d\lambda}{\int_0^\infty E_{b\lambda}\, d\lambda} \tag{24}$$

$$e_{ef} = \frac{\int_0^\infty e_{ef_\lambda} E_{b\lambda} d\lambda}{\int_0^\infty E_{b\lambda}\, d\lambda} \tag{25}$$

in which $E_{b\lambda}$ is Planck's distribution function evaluated at 10,460°R to simulate solar irradiation in Eq. (24) and is Planck's distribution function evaluated at 585°R for emittance in Eq. (25).

$$E_{b\lambda} = \frac{c_1 \lambda^{-5}}{e^{c_2/T\lambda} - 1} \tag{26}$$

The integrated reflectance and emittance factors calculated from Eqs. (24) and (25) are shown in Fig. 11.

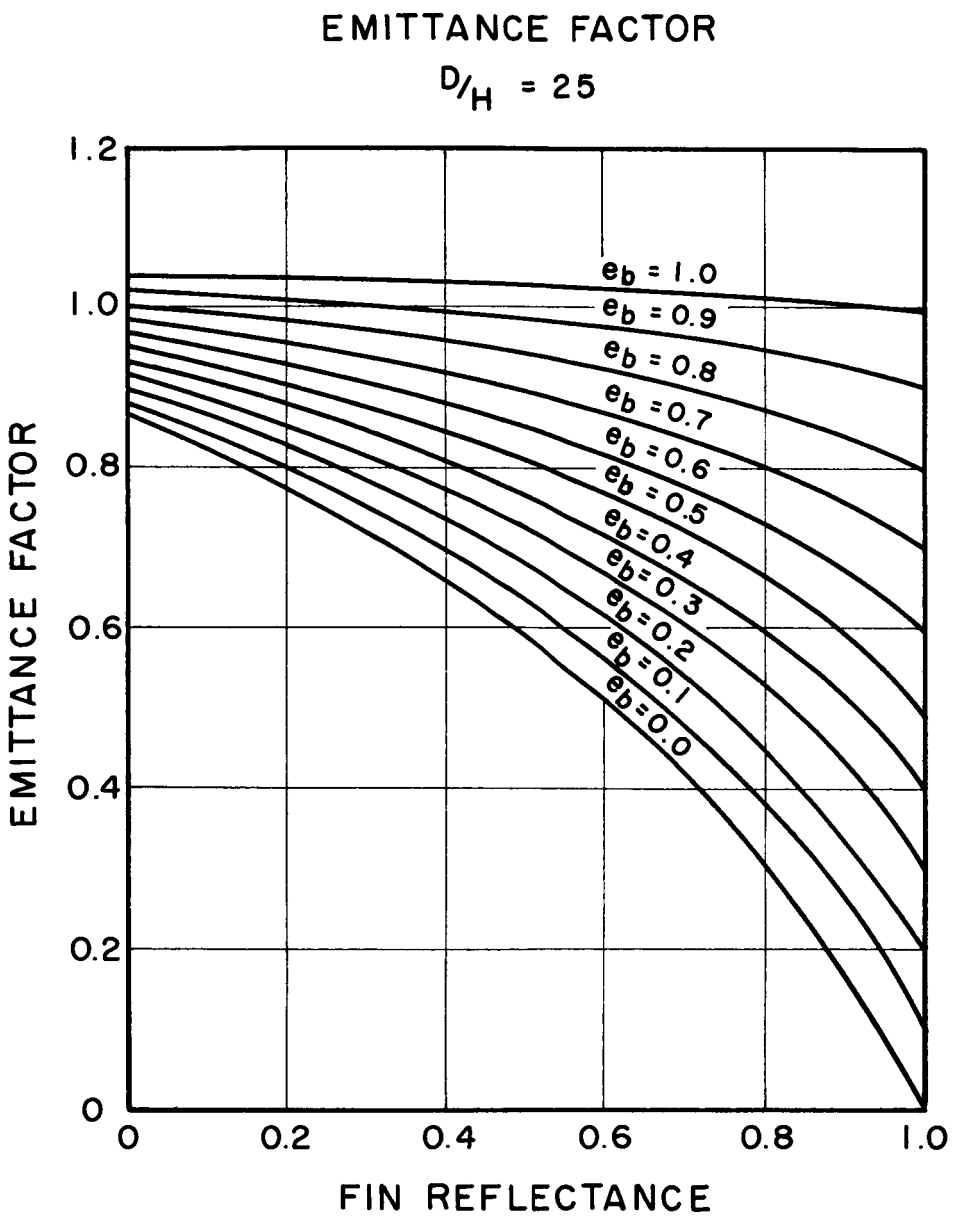
EMITTANCE FACTOR
D/H = 25
EMITTANCE FACTOR
FIN REFLECTANCE
1.2
1.0
0.8
0.6
0.4
0.2
0
0
0.2
0.4
0.6
0.8
1.0
eb = 1.0
eb = 0.9
eb = 0.8
eb = 0.7
eb = 0.6
eb = 0.5
eb = 0.4
eb = 0.3
eb = 0.2
eb = 0.1
eb = 0.0

Figure (9)

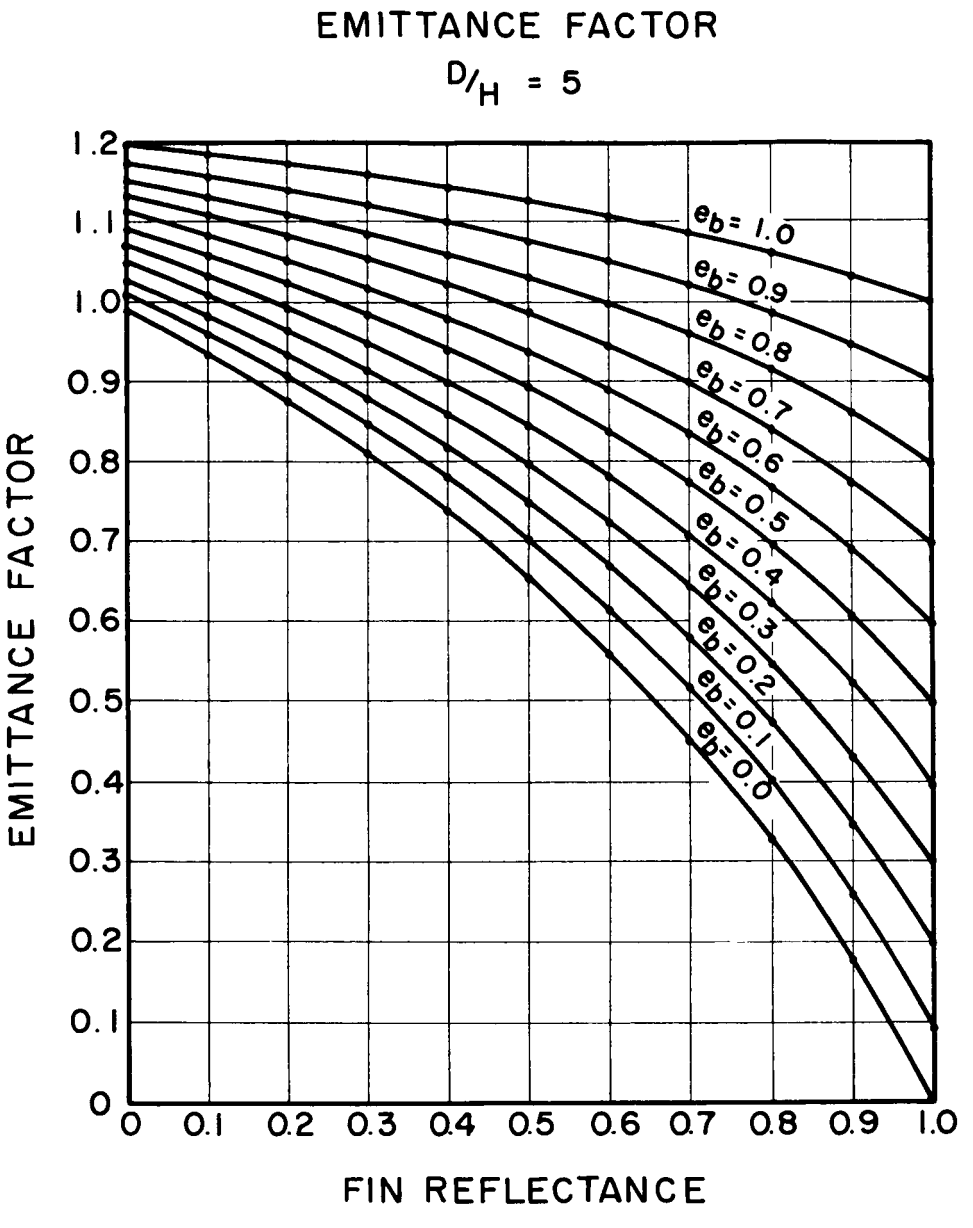
EMITTANCE FACTOR
D/H = 5
EMITTANCE FACTOR
1.2
1.1
1.0
0.9
0.8
0.7
0.6
0.5
0.4
0.3
0.2
0.1
0
0 0.1 0.2 0.3 0.4 0.5 0.6 0.7 0.8 0.9 1.0
FIN REFLECTANCE
eb= 1.0
eb= 0.9
eb= 0.8
eb= 0.7
eb= 0.6
eb= 0.5
eb= 0.4
eb= 0.3
eb= 0.2
eb= 0.1
eb= 0.0

Figure (10)

Calculation of e'_r

Assumptions
1) The fins always remain vertical
2) The fins are uniformly at the base temperature whether emitting or not
3) The slit between the adjacent thermostatic strips which form a fin is black
4) The base surface emits and reflects energy diffusely
5) The fins can emit diffusely and reflect specularly

The net heat flux from the spacecraft will be given by a modified form of Eq. (1) which takes into consideration the change in solar irradiation with solar polar angle and the changes in solar absorptance and surface emittance with temperature and solar polar angle

$$e'_r(\varphi,T_s) = e(T_s) - \alpha_s(\varphi,T_s)\,\frac{S\cos\varphi}{\sigma T_s^4} \qquad (27)$$

One can see in Fig. 1 how the incoming energy from the sun can strike the surface and 1) enter the groove between the fins, 2) enter the slit formed by the adjacent thermostat elements, or 3) strike the top of the fins. The areas of the first two depend upon the temperature of the spacecraft surface because of the thermostatic action of the fins.

The horizontal displacement of the top of one thermostatic element will be

$$d = \frac{(113 \times 10^{-7})\,(T_2 - T_1)\,H^2}{t} \qquad (28)$$

where t is the thickness of the thermostatic element
T_2-T_1 is the temperature change of the fin in °R
H is the height of the fin
d the displacement in inches.
Thus, the slit area is directly proportioned to 2d.

The area of the groove is equal to the total area minus the area of the slit and fin top. The ratio A_G/A_{TOT} is the fraction of the surface which will allow the incoming radiation to strike the white base.

$$\frac{A_G}{A_{TOT}} = 1 - \frac{2t}{w + 2t} - \frac{2(113 \times 10^{-7})\,(T_2 - T_1)H^2}{t(w + 2t)} \qquad (29)$$

where w = distance between fins.

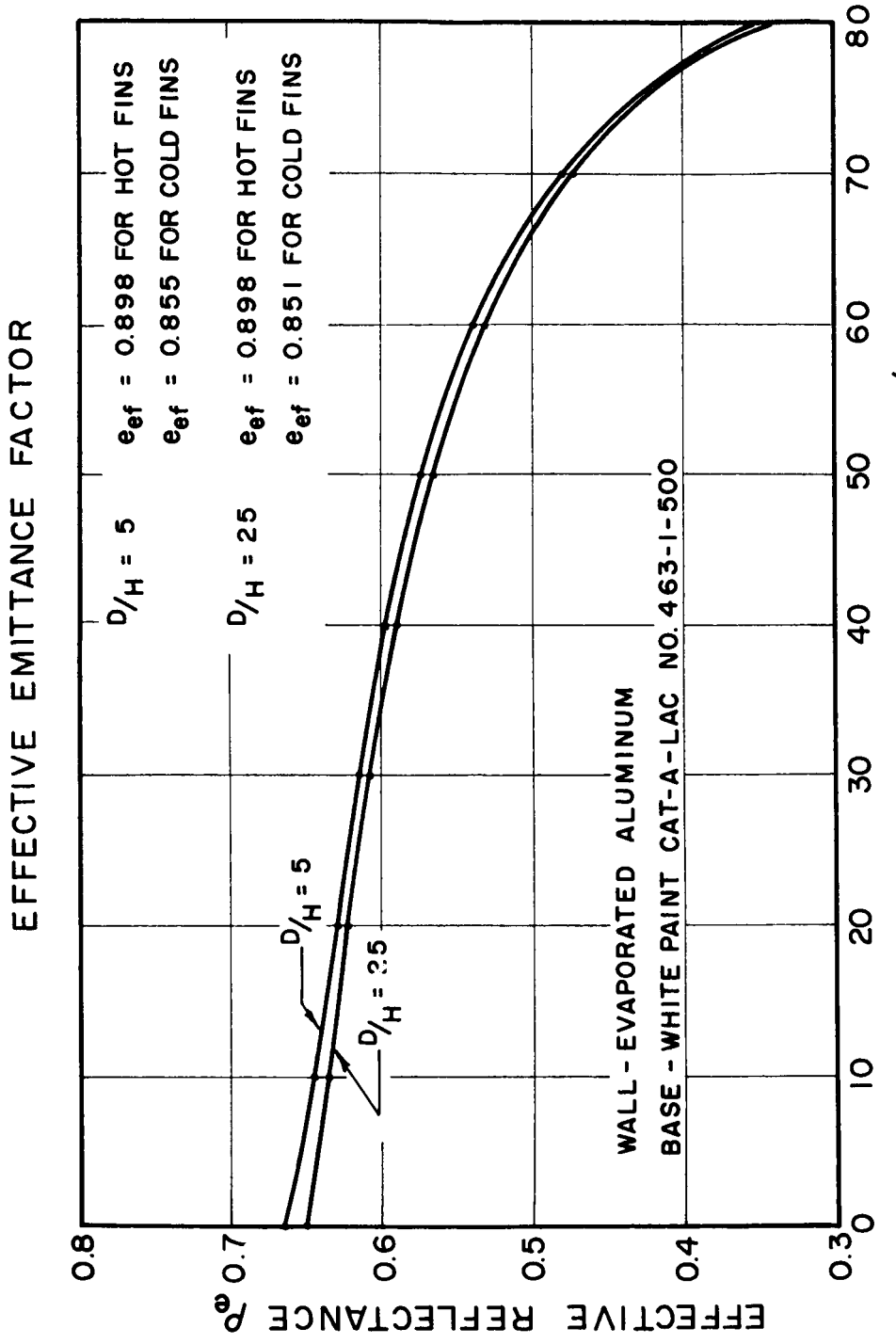
EFFECTIVE EMITTANCE FACTOR
$D/H = 5$ $e_{ef} = 0.898$ FOR HOT FINS
$e_{ef} = 0.855$ FOR COLD FINS
$D/H = 25$ $e_{ef} = 0.898$ FOR HOT FINS
$e_{ef} = 0.851$ FOR COLD FINS
$D/H = 5$
$D/H = 25$
WALL - EVAPORATED ALUMINUM
BASE - WHITE PAINT CAT-A-LAC NO. 463-1-500
EFFECTIVE REFLECTANCE ρ_ϕ
0.8
0.7
0.6
0.5
0.4
0.3
0
10
20
30
40
50
60
70
80
SOLAR POLAR ANGLE ϕ

Figure (11)

The area of the slit A_{SL} is simply the distance between the adjacent thermostatic elements.

$$\frac{A_{SL}}{A_{TOT}} = \frac{2(133 \times 10^{-7})\ (T_2 - T_1)H^2}{t(w + 2t)} \tag{30}$$

The area of the top A_{TOP} is equal to twice the thickness of the thermostatic element.

$$\frac{A_{TOP}}{A_{TOT}} = \frac{2t}{w + 2t} \tag{31}$$

Eqs. (29,30,31) are fractions of the total area which have the radiant characteristics of the slit, groove or thermostatic fin top. The effective emissivity of the surface will, therefore, be equal to the sum of the emissivities of the three areas times their area fractions.

$$e_e = \frac{A_{TOP}}{A_{TOT}}\ e_{TOP} + \frac{A_{SL}}{A_{TOT}}\ e_{SL} + \frac{A_G}{A_{TOT}}\ e_G \tag{32}$$

and similarly for absorptance.

$$\alpha_s = \frac{A_{TOP}}{A_{TOT}}\ \alpha_{TOP} + \frac{A_{SL}}{A_{TOT}}\ \alpha_{SL} + \frac{A_G}{A_{TOT}}\ \alpha_G \tag{33}$$

In the calculations which were made for this report, the following assumptions were used in the evaluation of e_e and α_s.

1) $e_{TOP} = \alpha_{TOP} = .1$ independent of temperature

2) $e_{SL} = \alpha_{SL} = 1.0$, independent of temperature

3) $e_G = f(\rho_b, \rho_w) =$ constant

4) $\alpha_G = 1 - \rho_e(\varphi)$, independent of temperature.

The last three assumptions are quite good when the temperature of the surface deviates only a few degrees from the temperature (T_2) at which the fins are perpendicular to the white base surface. However, as the surface turns away from the sun and gets colder, the opening over the white groove becomes smaller and its emittance and absorptance both approach one. At the same time, the slit is opening exposing a metallic surface to space decreasing its emittance and absorptivity.

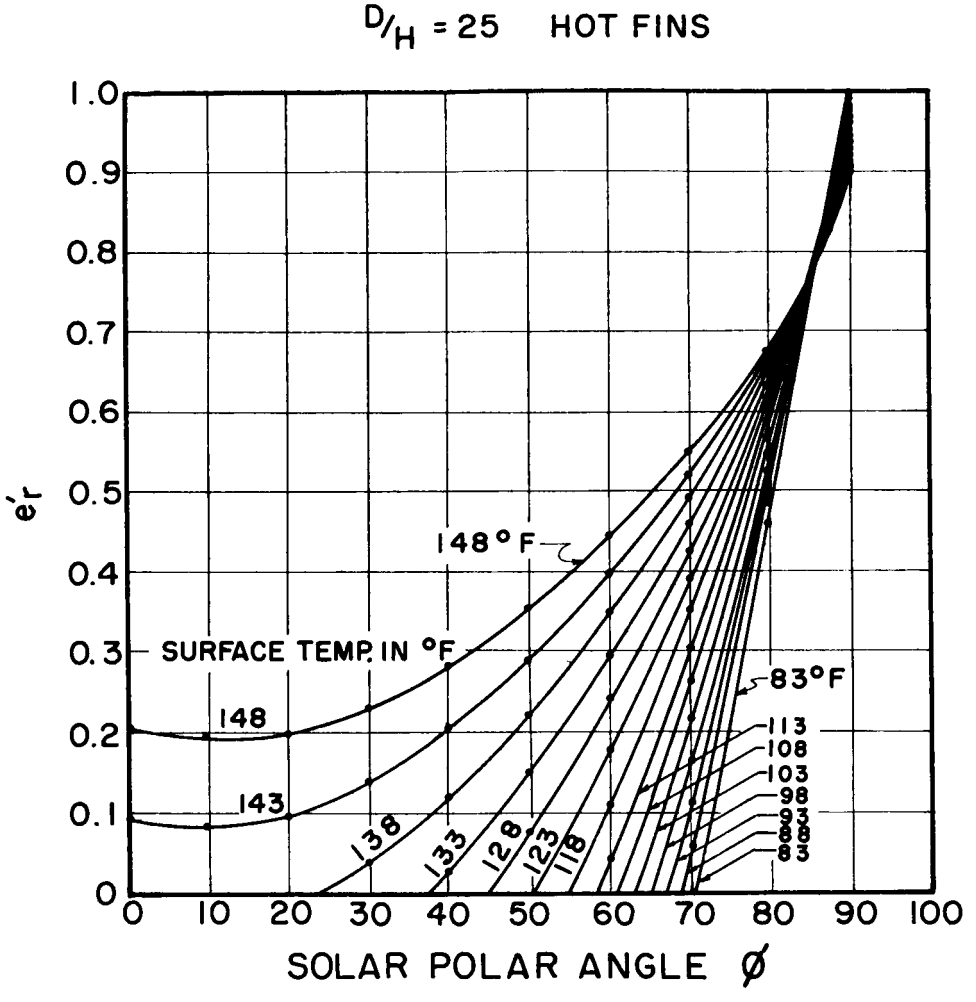
D/H = 25 HOT FINS
1.0
0.9
0.8
0.7
0.6
0.5
0.4
0.3
0.2
0.1
0
e'r
148°F
SURFACE TEMP. IN °F
148
143
138
133
128
123
118
113
108
103
98
93
88
83
83°F
0 10 20 30 40 50 60 70 80 90 100
SOLAR POLAR ANGLE Ø

Figure (12)

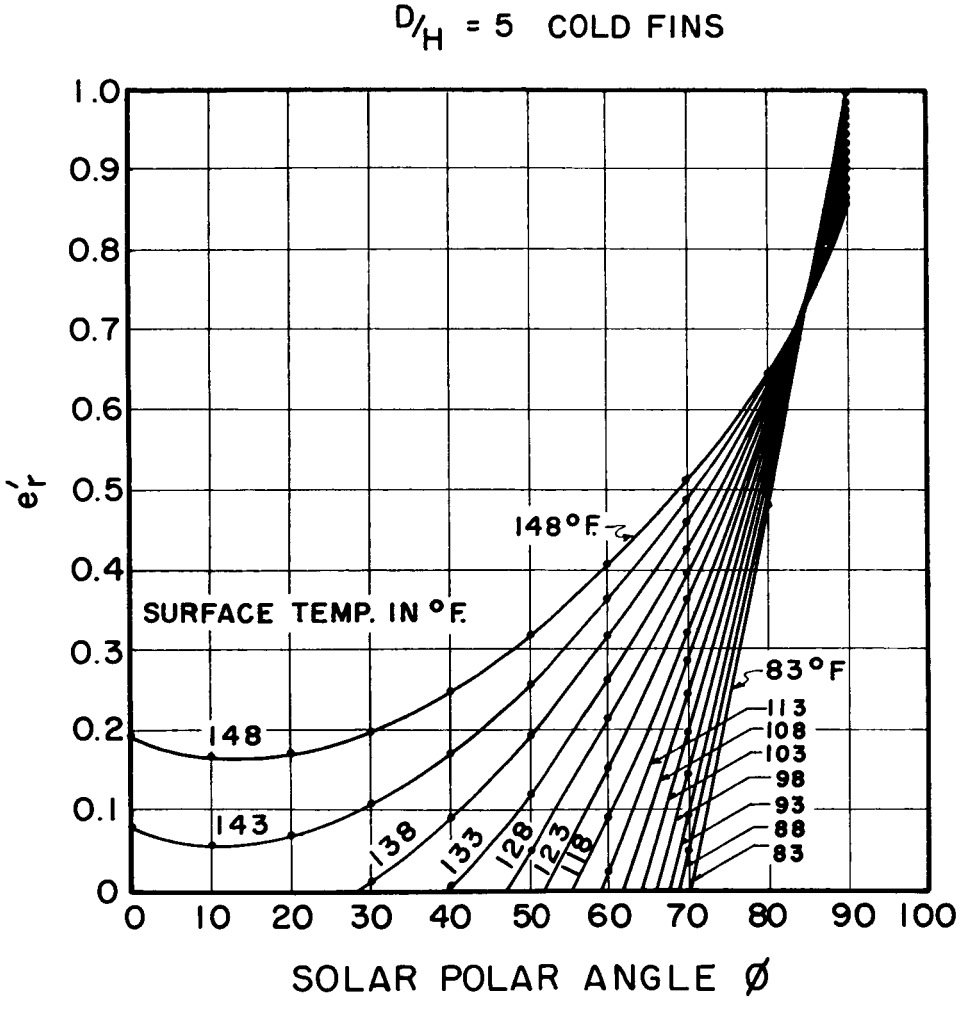
D/H = 5 COLD FINS
1.0
0.9
0.8
0.7
0.6
0.5
0.4
0.3
0.2
0.1
0
e'r
SURFACE TEMP. IN °F.
148°F.
148
143
138
133
128
123
118
83°F
113
108
103
98
93
88
83
0 10 20 30 40 50 60 70 80 90 100
SOLAR POLAR ANGLE Ø

Figure (13)

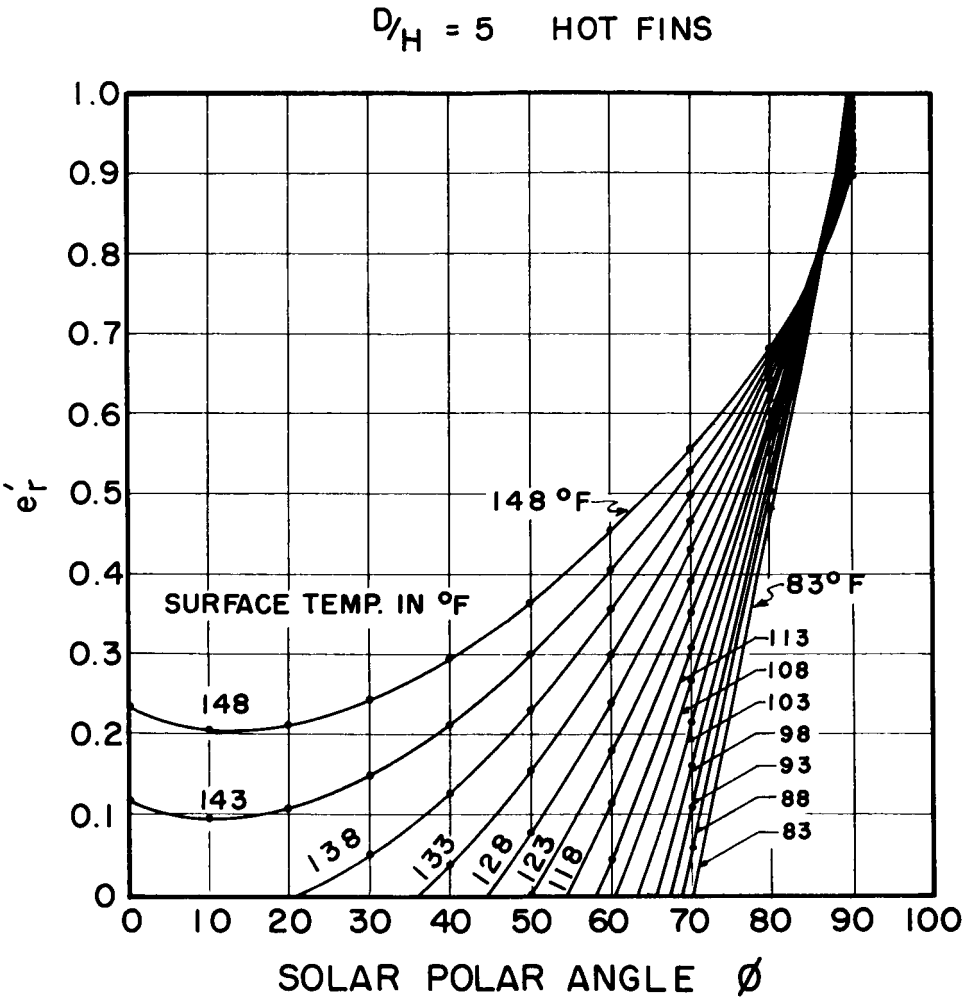
D/H = 5 HOT FINS
1.0
0.9
0.8
0.7
0.6
0.5
0.4
0.3
0.2
0.1
0
e'r
148 °F
83° F
SURFACE TEMP. IN °F
148
143
138
133
128
123
118
113
108
103
98
93
88
83
0 10 20 30 40 50 60 70 80 90 100
SOLAR POLAR ANGLE Ø

Figure (14)

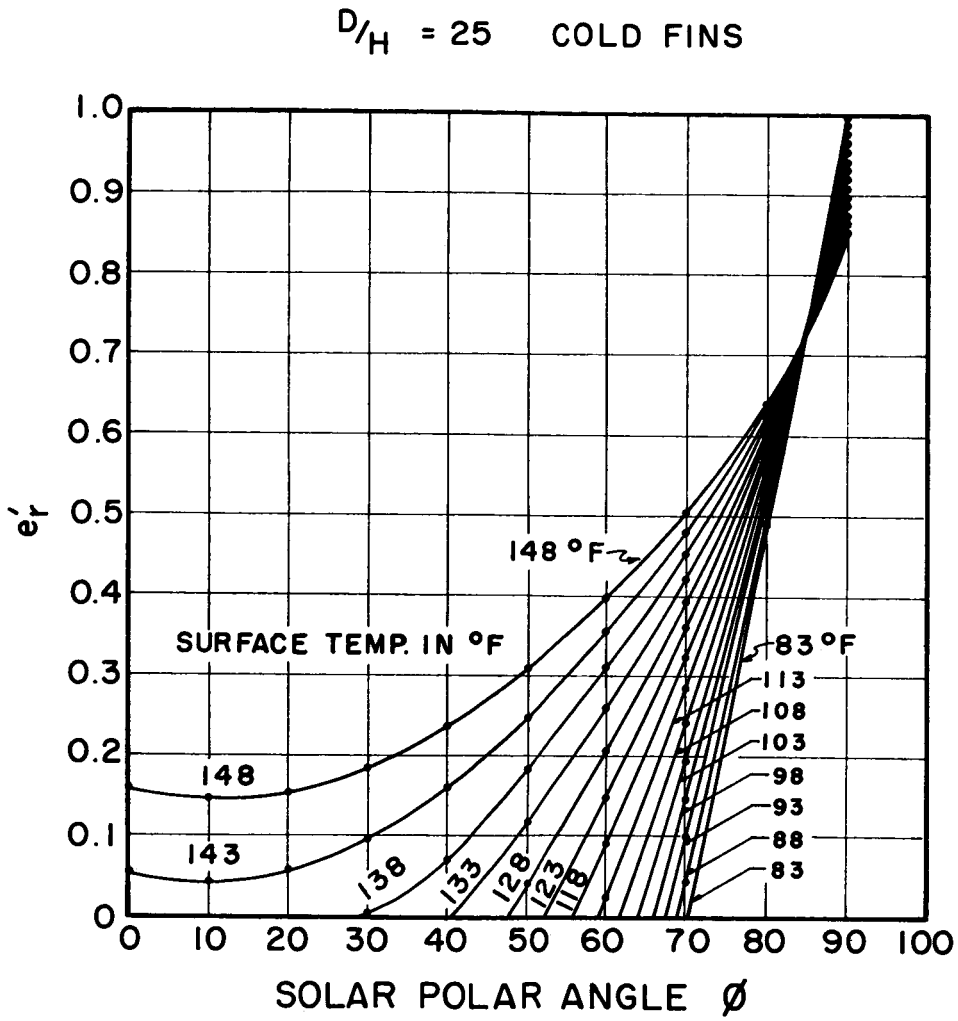
D/H = 25 COLD FINS
1.0
0.9
0.8
0.7
0.6
0.5
0.4
0.3
0.2
0.1
0
e'r
148 °F
SURFACE TEMP. IN °F
83 °F
113
108
103
98
93
88
83
148
143
138
133
128
123
118
0 10 20 30 40 50 60 70 80 90 100
SOLAR POLAR ANGLE Ø

Figure (15)

For this reason, Eqs. (32) and (33) are only good up to a solar polar angle of about 80°. e'_r as calculated from Eq. (27) is shown in Figs. 12,13,14, and 15.

Experimental Phase of Project

The experimental phase of this project consists of the testing of a full scale model of the thermostatic spacecraft in a space simulator surface and the measurement of the reflectance properties of both the fin material and base material.

Description of Model

The model consists of a 12" x 12" x 1/8" aluminum plate on which 5 rows of 2" long fins are mounted so that they are perpendicular to the surface and stand 2" apart. The aluminum base material is painted with Cat-a-lac white epoxy paint. (See Fig. 16).

Directly behind the sample surface is a heater which is used to maintain a specified heat flux through the surface. The sample surface and heater combination are insulated on the sides and rear such that the heat transferred is assumed to travel only through the sample surface. Provisions are made to measure surface and heater temperatures with iron constantan thermocouples and the heater power dissipation with a wattmeter. The sample will be placed in a solar simulator and the temperature of the surface measured as a function of solar polar angle and heat flux.

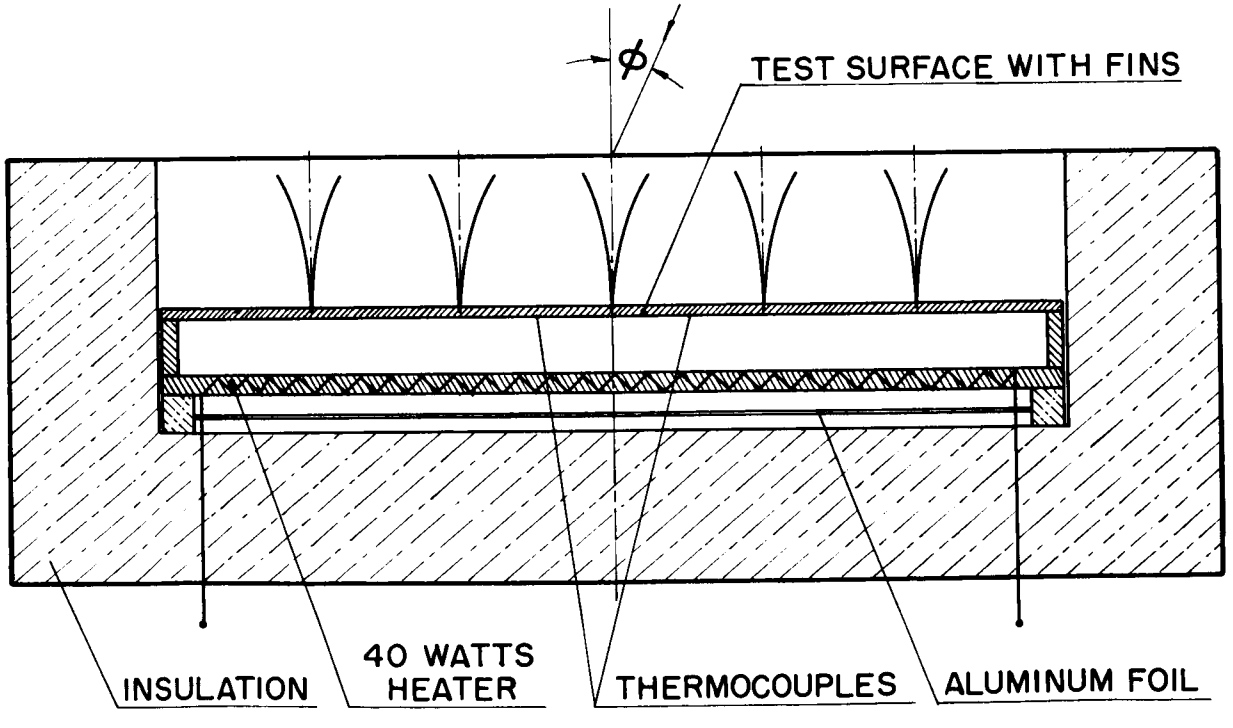

Figure (16)

Integrating Sphere Reflectometer

In order to determine the monochromatic reflectance characteristics of the thermostatic fin material and the base coating an integrating sphere reflectometer was constructed, Fig. 17. The integrating sphere is based on the principle that the view factor from any point on the white, diffuse wall of the sphere (a) to the detector (b) is the same as from any other point to the detector. Thus, a detector placed in a position underneath the sample (c) "sees" and registers in proportion to the amount of energy reflected from the sample onto the sphere wall. When the sample is removed from the path of the incoming beam, then the wall is illuminated directly (d) and the detector registers in proportion to the amount of energy which was incident upon the sample. The reflectance is then the ratio of the two detector outputs. The sphere should yield values correct to 1 %. A complete error analysis and description of the many uses of the integrating sphere is given in Ref. [3]. Measurements made on the fin material are shown in Fig. 18.

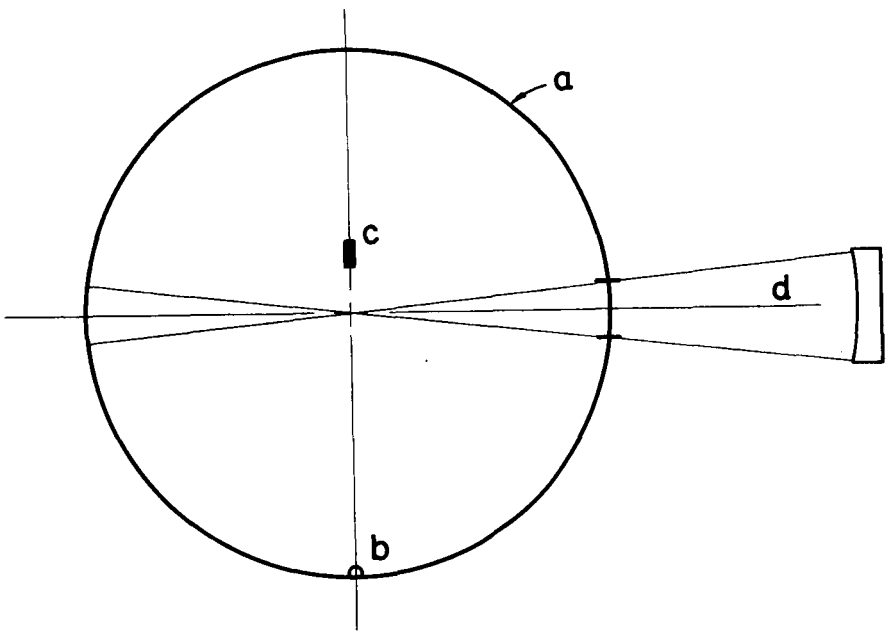

Figure (17)

RESULTS

From the information contained in Figs. 12-15 the spacecraft equilibrium temperatures were calculated which would yield a net heat loss of 37.5 Btu/Hr-Ft^2 of spacecraft surface. The surface temperatures obtained for both hot (emitting) and cold (nonemitting)fins are shown in Figs. 20 and 21. The dashed line in these figures represents an approximation to the correct equilibrium temperatures which will be obtained when the walls have deviated from their vertical position so that the emittance of the slit is low and the emittance of the groove is higher than was calculated by Eq. (16). It is also apparent that there was little difference in the equilibrium temperatures obtained with either hot or cold fin and D/H ratios of 5 or 25. This indicates that conduction effects and end losses can be ignored for evaporated aluminum fins and D/H ratios greater than 5.

CONCLUSIONS AND RECOMMENDATIONS

The analysis shows that short fins still provide adequate control of spacecraft surface temperature. It is recommended that a design procedure be devised which would yield H/W ratios, fin reactiveness, fin height, and surface coatings based on mission program, heat dissipation requirements and temperature excursion limits.

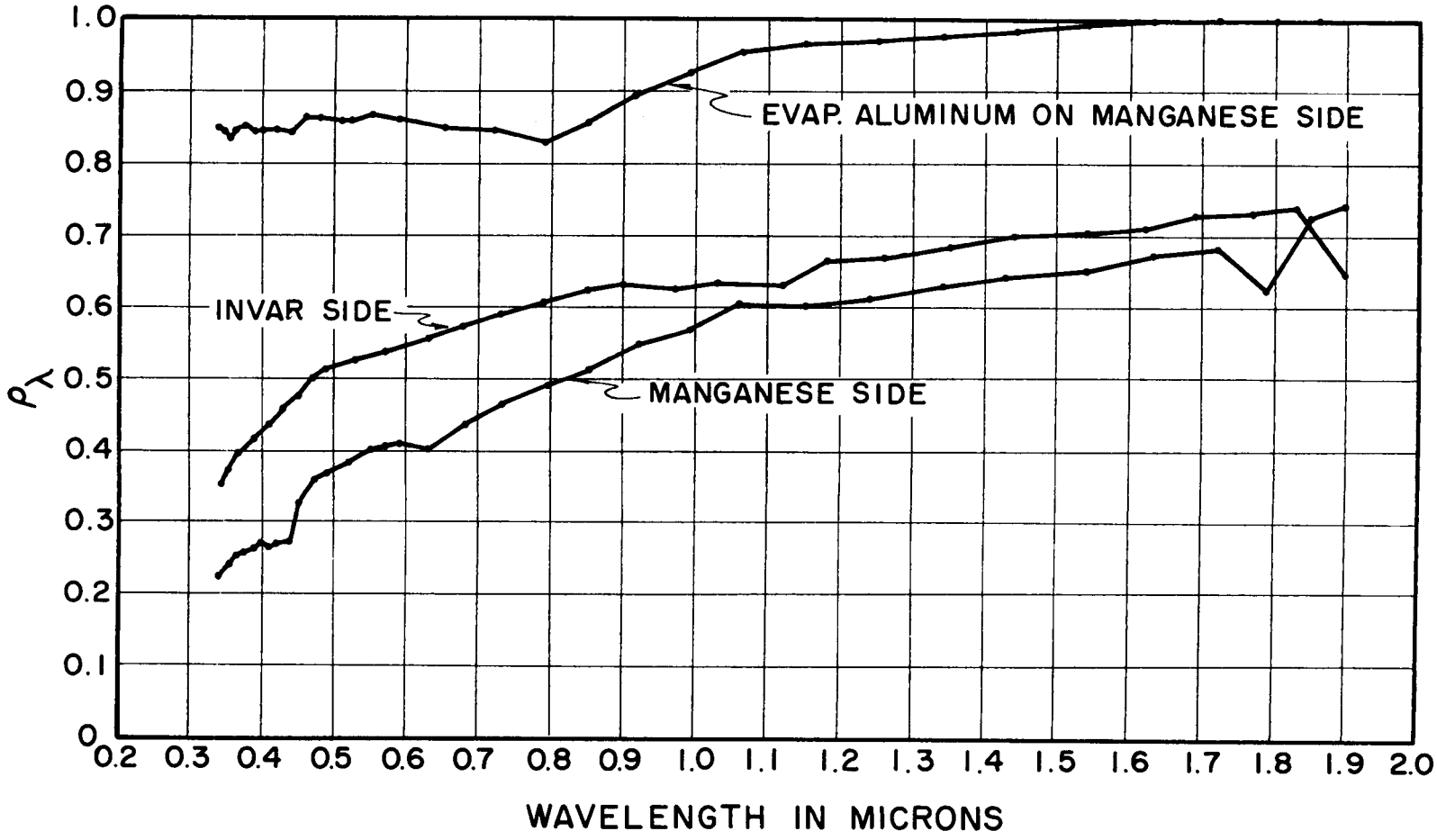
1.0
0.9
0.8
0.7
0.6
0.5
0.4
0.3
0.2
0.1
0
ρ_λ
EVAP. ALUMINUM ON MANGANESE SIDE
INVAR SIDE
MANGANESE SIDE
0.2 0.3 0.4 0.5 0.6 0.7 0.8 0.9 1.0 1.1 1.2 1.3 1.4 1.5 1.6 1.7 1.8 1.9 2.0
WAVELENGTH IN MICRONS

Figure (18)

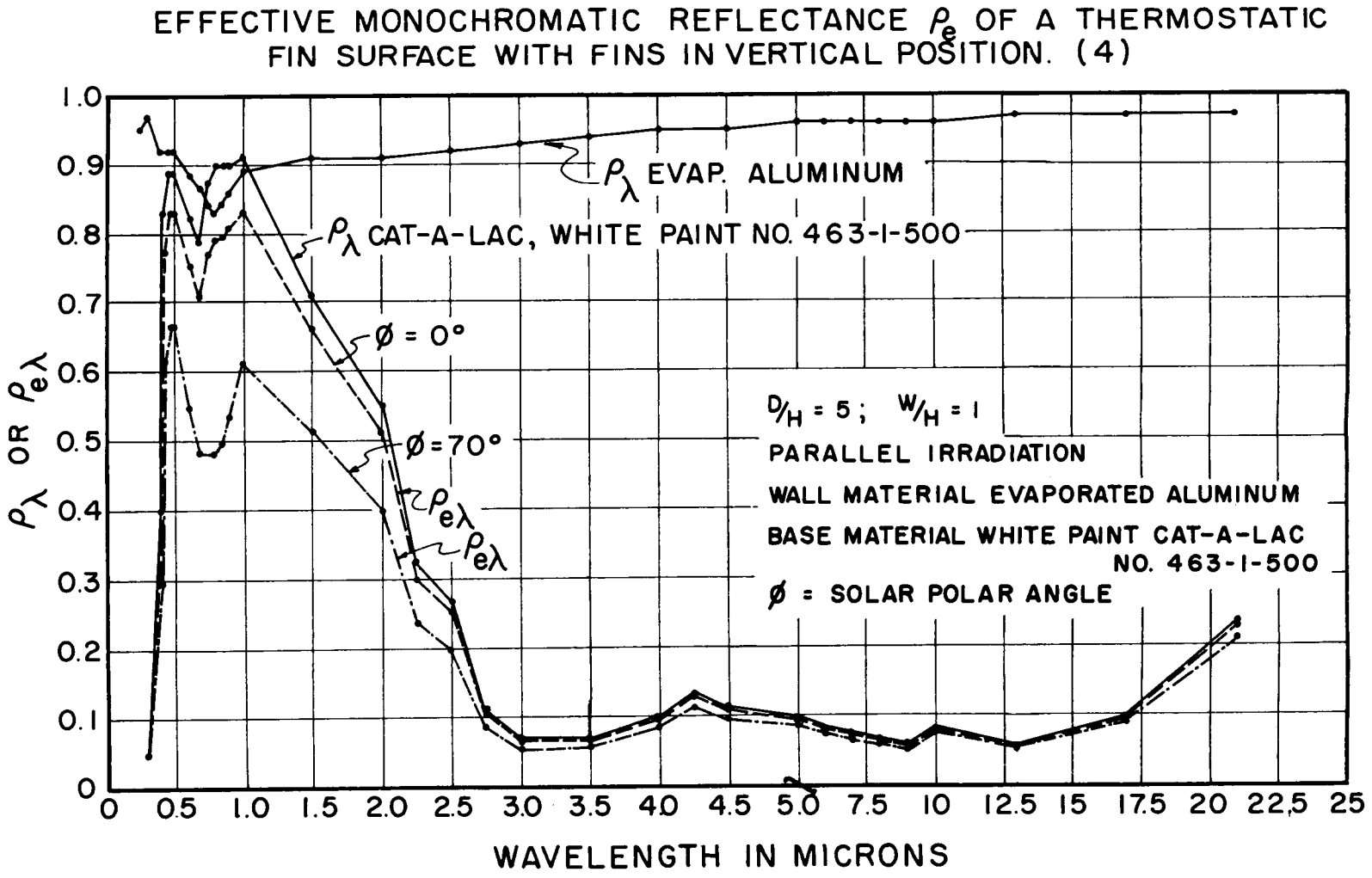
EFFECTIVE MONOCHROMATIC REFLECTANCE ρ_e OF A THERMOSTATIC FIN SURFACE WITH FINS IN VERTICAL POSITION. (4)
ρ_λ EVAP. ALUMINUM
ρ_λ CAT-A-LAC, WHITE PAINT NO. 463-1-500
$\phi = 0°$
$\phi = 70°$
$\rho_{e\lambda}$
$\rho_{e\lambda}$
$D/H = 5$; $W/H = 1$
PARALLEL IRRADIATION
WALL MATERIAL EVAPORATED ALUMINUM
BASE MATERIAL WHITE PAINT CAT-A-LAC NO. 463-1-500
ϕ = SOLAR POLAR ANGLE
ρ_λ OR $\rho_{e\lambda}$
1.0
0.9
0.8
0.7
0.6
0.5
0.4
0.3
0.2
0.1
0
0 0.5 1.0 1.5 2.0 2.5 3.0 3.5 4.0 4.5 5.0 7.5 10 12.5 15 17.5 20 22.5 25
WAVELENGTH IN MICRONS

Figure (19)

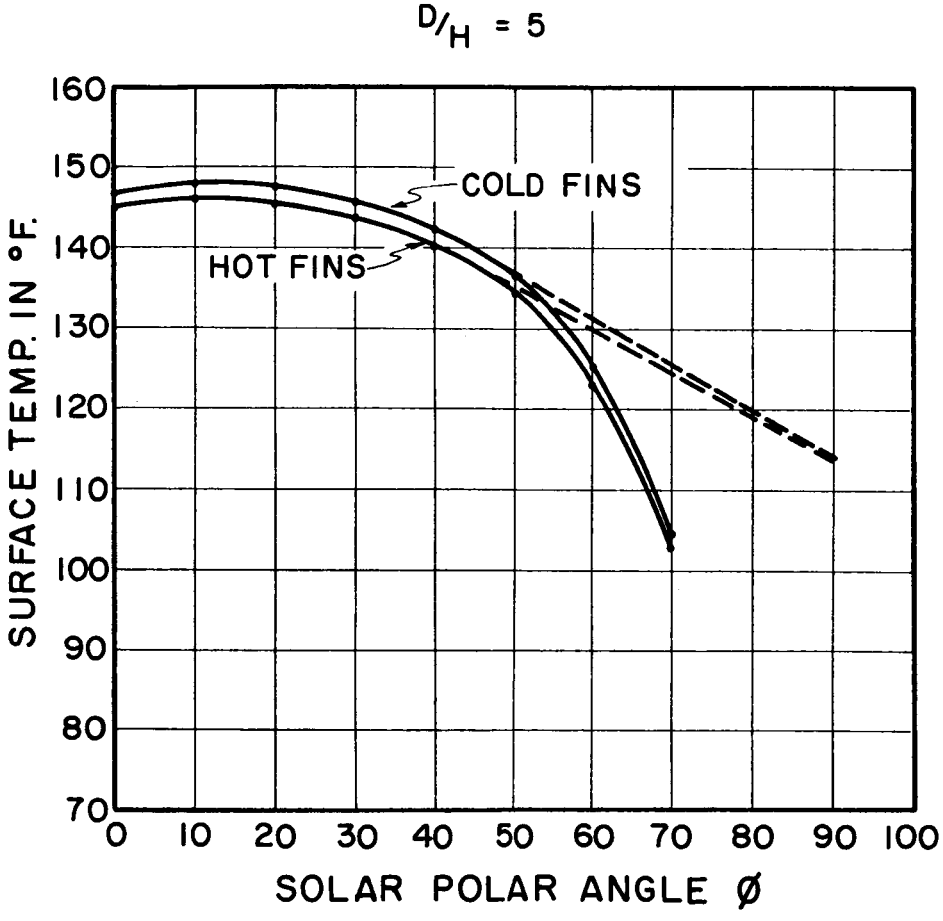
D/H = 5
160
150
140
130
120
110
100
90
80
70
SURFACE TEMP. IN °F.
COLD FINS
HOT FINS
0
10
20
30
40
50
60
70
80
90
100
SOLAR POLAR ANGLE Ø

Figure (20)

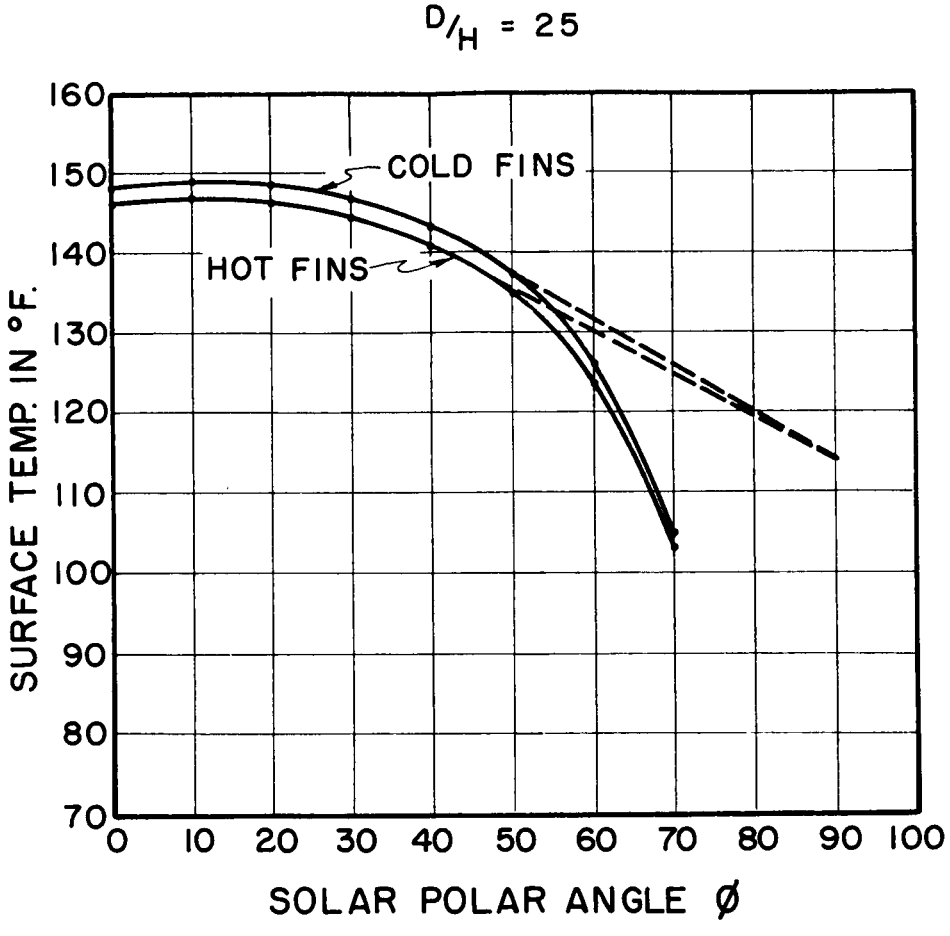
D/H = 25
160
150
140
130
120
110
100
90
80
70
COLD FINS
HOT FINS
SURFACE TEMP. IN °F.
0
10
20
30
40
50
60
70
80
90
100
SOLAR POLAR ANGLE Ø

Figure (21)

BIBLIOGRAPHY

[1] Wiebelt, J. A., J. F. Parmer, "Spacecraft Temperature Control by Thermostatic Fins-Analysis", NASA Contractor Report, NASA CR-91.

[2] Hamilton, D. C. and W. R. Morgan, "Radiant Interchange Configuration Factors", NACA-TN-2836, December 1952.

[3] Edwards, D. K., J. T. Gier, K. E. Nelson, R. D. Roddick, Integrating Sphere for Imperfectly Diffuse Samples", Applied Optics, V51; November, 1961.

[4] Edwards, D. K., K. E. Nelson, R. D. Roddick, and J. T. Gier, "Basic Studies on the Use and Control of Solar Energy", Report No. 60-93, October, 1960, NSF-G-9505.